Original research paper

Combined shake-flask, chromatographic and *in silico* approaches for evaluating the physicochemical and ADME properties of aloin A and aloe-emodin

DANIELA AMIDŽIĆ KLARIĆ[1]
JELENA KOVAČIĆ[1]
PETRA BAJT[2]
NIKŠA TURK[3]
ŽELJKO KRZNARIĆ[3,4]
EMMA RIORDAN[5]
ANA MORNAR[1,*]

[1] *Department of Pharmaceutical Analysis, Faculty of Pharmacy and Biochemistry, University of Zagreb, 10000 Zagreb, Croatia*

[2] *Center for Translational Research and Innovation in Pharmacy, Faculty of Pharmacy and Biochemistry, University of Zagreb, 10000 Zagreb, Croatia*

[3] *Department of Gastroenterology, University Hospital Centre, 10000 Zagreb, Croatia*

[4] *School of Medicine, University of Zagreb, 10000 Zagreb Croatia*

[5] *School of Pharmacy, University College Cork, T12 YT20 Cork, Ireland*

ABSTRACT

Aloe vera has a long history of medicinal use due to its diverse biological activities, including antioxidant, anti-inflammatory and antimicrobial. This study investigates the physicochemical and ADME (absorption, distribution, metabolism, excretion) properties of two primary anthraquinones from *Aloe vera*, aloin A and aloe-emodin. The focus of this research was to evaluate the lipophilicity, solubility, and pharmacokinetic profiles of aloin A and aloe-emodin through a combination of computational predictions, the shake-flask method, and chromatographic techniques. The optimised shake-flask method was successfully employed to determine the log P values of phytochemicals. Aloin A was found to be more hydrophilic than aloe-emodin, likely due to the presence of an attached β-ᴅ-glucopyranosyl unit. All RP-TLC and RP-HPLC lipophilicity indices were higher for aloe-emodin compared to aloin A, aligning with their log P values (obtained through *in silico* and shake-flask methods). IAM (immobilised artificial membrane)-HPLC results suggest that unlikely partitioning in the *n*-octanol/water system or C18 chains, partition into phospholipids involves not only hydrophobic intermolecular recognition forces but also electrostatic interactions. The presence of a sugar moiety (β-ᴅ-glucopyranosyl unit) at the C-10 position of aloin A considerably enhanced its affinity to phospholipids compared to its affinity to alkyl chains. HSA (human serum albumin)-HPLC and AGP (α1-acid glycoprotein)-HPLC data confirmed aloe-emodin's stronger affinity to plasma proteins. The integration of computational and experimental approaches provided a detailed understanding of aloin A and aloe-emodin physicochemical and ADME properties.

Keywords: *Aloe vera*, aloin A, aloe-emodin, ADME properties, lipophilicity, biomimetic chromatography

INTRODUCTION

Aloe vera (L.) Burm.f. (Asphodelaceae), including *A. vera* and *A. maculata*, grows in tropical climates throughout the world. Depending on the species, the influence of climatic and growing conditions, and the diversity of the ecosystem to which they belong, the

---

* Correspondence; ana.mornar@pharma.unizg.hr

phytochemical constituents can be different in *Aloe vera* plants, containing over 75 nutrients and 200 biologically active constituents, including hydrosoluble and liposoluble vitamins, enzymes, minerals and sugars. Moreover, it contains anthraquinones, fatty acids and hormones (1–6).

Anthraquinones (9,10-dioxoanthracenes or anthracenediones) are a class of polycyclic compounds with a quinoid structure. Natural anthraquinones have the most common structure of 9,10-anthraquinone with three rings, of A, B and C, as the basic skeleton. If the parent nucleus of anthraquinone is substituted with hydroxyl, hydroxymethyl, methyl, methoxyl or carboxy group, free anthraquinone can be formed, which, when combined with glucoside, gentiobioside and primeveroside, forms glycosides of conjugated anthraquinones. Anthraquinones, synthesised *via* the acetate-polymalonate pathway or the shikimic acid-*O*-succinyl benzoic acid-mevalonic acid pathway, are the major bioactive components of aloe.

The primary anthraquinone derivatives present in *Aloe vera* are aloin and aloe-emodin (Fig. 1) (1, 7). Aloin ($C_{21}H_{22}O_9$) belongs to a class of anthraquinones and anthrones. Anthrones (9,10-dihydro-9-oxo-anthracene) are anthracene derivatives that feature a single carbonyl group at the C-9 position and lack a carbonyl group at the C-10 position. Aloin consists of a chromone nucleus (an anthracene derivative) linked to a sugar moiety (β-D-glucopyranosyl unit) at the C-10 position. It exists in two stereoisomeric forms: aloin A (barbaloin) and aloin B (isobarbaloin), which differ in the configuration of the glycosidic bond. Aloin A represents the (10*S*) enantiomer, while aloin B corresponds to the (10*R*) enantiomer (5, 7). Aloe-emodin ($C_{15}H_{10}O_5$), on the other hand, is a dihydroxyanthraquinone derivative. It is a chrysazin molecule that carries a hydroxymethyl group at the C-3 position.

The characterisation of the physicochemical properties of putative drug molecules and new chemical entities is a critical step in the drug design process. Among the most significant properties are lipophilicity, phospholipid binding, and protein binding.
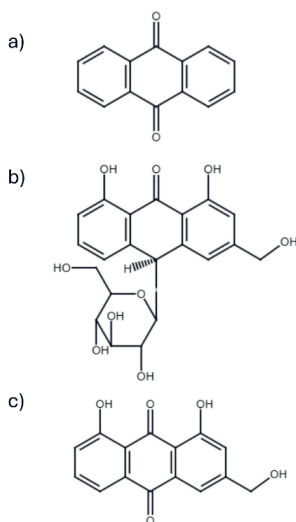

Fig. 1. Structure of: a) anthraquinone, b) aloin A and c) aloe-emodin.

Traditionally, *n*-octanol/water partition coefficients, determined using the shake-flask method, have been employed to model biological partitioning processes. However, this approach has notable drawbacks, including labour-intensive sample preparation and environmental concerns. As a result, there is an increasing demand for alternative methods capable of estimating lipophilicity more efficiently. Chromatographic techniques offer a valuable alternative for evaluating hydrophobicity, lipophilicity, phospholipid binding, and protein binding. Over the last two decades, computational chemistry and *in silico* approaches have undergone significant advancements, transforming the prediction of physicochemical and ADME (absorption, distribution, metabolism, excretion) properties for putative drug molecules and new chemical entities. These advancements have been driven by improvements in computational power, algorithm development, and the availability of extensive datasets for model training. In particular, the emergence of artificial intelligence, machine learning and deep learning methods have enabled the development of highly accurate predictive models based on the molecular structure of various compounds (8–14).

Despite the widespread use of *Aloe* and its products, there is limited *in silico* data available regarding the physicochemical and ADME properties of its biologically active compounds (15–18). This lack of data is a common phenomenon for many other phytochemicals as well.

Herein, we report a comprehensive study on the primary *Aloe vera* phytochemicals, aloin A and aloe-emodin, encompassing: (*i*) physicochemical and ADME properties predicted through *in silico* methods, (*ii*) *n*-octanol/buffer partition coefficients determined using the shake-flask method with automated sampling, (*iii*) lipophilicity indices obtained *via* reversed-phase chromatography, (*iv*) affinity to immobilized artificial membranes (IAM), and (*v*) plasma protein binding evaluated through biomimetic chromatography.

EXPERIMENTAL

Chemicals

Aloin A (USP Reference Standard) was obtained from Sigma-Aldrich (USA), while aloe-emodin (Primary Reference Standard, Phyproof® Reference Substance) was purchased from Merck KGaA (Germany). Buffer solutions were prepared using phosphate-buffered saline (PBS) tablets (Sigma-Aldrich), disodium hydrogen phosphate dihydrate (buffer substance for chromatography) and sodium dihydrogen phosphate dihydrate (EMSURE® reagent Ph. Eur.), both supplied by Merck. Organic solvents, including *n*-octanol (gradient grade for liquid chromatography, ≥ 99 %) and methanol (gradient grade for liquid chromatography LiChrosolv® Reag. Ph Eur.), as well as formic acid (for LC-MS, LiChropur®, 97.5–98.5 %) and dimethyl sulfoxide (DMSO) (suitable for HPLC, ≥ 99.7 %), were purchased from Merck. The dead volume of RP- and IAM-HPLC systems was evaluated using sodium nitrate (reagent for USP/NF monographs) from J. T. Baker (USA).

Instruments

All high-performance liquid chromatography (HPLC) measurements were performed on an Agilent 1260 series HPLC system (Agilent Technologies, USA), consisting of the

following modular components: a vacuum degassing unit, a binary pump, an automatic sample injector with drawer kit for 40 × 2 mL vials, a column oven, and a diode array detector. System control, data acquisition, and data processing were managed using OpenLab ChemStation software (Agilent Technologies).

Additional laboratory equipment included an Elmasonic XtraTT ultrasonic bath (Elma Schmidbauer, Germany), an ES-20/60 shake-incubator (Biosan, Latvia), a Z 326 K tabletop centrifuge (HERMLE Labortechnik, Germany), and a UV Cabinet with a Dual Wavelength UV Lamp (Camag, Switzerland).

Ultra-pure water with a resistivity of 18.2 MΩ·cm at 25 °C, obtained from the WaterPro water system (Labconco, USA), was used in all experiments.

Methods

In silico *calculations*. – Various software packages were utilised to calculate lipophilicity, each employing distinct algorithms. For each compound, 14 different log *P* values were generated using tools such as the Molecular Modeling Group's web service at the Swiss Institute of Bioinformatics (http://www.swissadme.ch), the Virtual Computational Chemistry Laboratory software (http://www.vcclab.org), Molinspiration Cheminformatics Group's free web service (https://www.molinspiration.com), Mcule, Inc.'s online platform (https://mcule.com/apps/property-calculator/), OSIRIS Property Explorer, part of Actelion's system (https://www.organic-chemistry.org/prog/peo/), Molsoft L.L.C.'s online tool (https://molsoft.com/mprop/), the pkCSM platform developed by the University of Melbourne and the University of Cambridge (http://biosig.unimelb.edu.au/pkcsm/), Preadmet QSARHUB web application for drug-likeness prediction (https://preadmet.qsarhub.com/druglikeness/), and preADMET web service from Yonsei University (https://preadmet.webservice.bmdrc.org/adme/).

Solubility predictions were performed using the aforementioned tools as well as admetSAR, an updated comprehensive tool (http://lmmd.ecust.edu.cn/admetsar2/).

Topological polar surface area (TPSA) values were calculated using six tools: Swiss ADME, Molinspiration, Mcule, OSIRIS Property Explorer, MolSoft, and pkCSM.

Advanced tools with diverse algorithms, including MolSoft, Preadmet QSARHUB, pkCSM, preADMET and admetSAR, were employed to evaluate ADME properties such as human intestinal absorption (HIA), skin permeability, plasma protein binding (PPB), and blood-brain barrier (BBB) permeability.

The molecular structures of the phytochemicals were converted into Simplified Molecular-Input Line-Entry System (SMILES) format, or the JME Molecular Editor tool was used to ensure accuracy in data processing.

Shake-flask method and chromatographic analysis

Sample preparation. – Stock solutions of aloin A and aloe-emodin were prepared in DMSO at a concentration of 2 mg mL^{-1}. Working solutions (from 0.1 to 5 µg mL^{-1}) were freshly prepared daily by diluting the stock solutions with 20 mmol L^{-1} PBS (pH 7.4) pre-saturated with *n*-octanol. Before analysis, all solutions were sonicated for 15 minutes at room temperature in an ultrasonic bath and subsequently filtered through 0.2-µm polyethersulfone filters (Obrnuta faza, Croatia).

To determine the logarithm of the partition coefficient (log P), pre-saturated *n*-octanol-PBS solutions (20 mmol L^{-1}, pH 7.4) were prepared by mutual saturation in a 1:1 (*V/V*) ratio. The solutions were shaken for 24 hours at 100 oscillations per minute in a shaker-incubator maintained at 25.0 ± 0.1 °C. The saturated mixtures were then allowed to rest for at least 12 hours in a thermostat set to 25.0 ± 0.1 °C to ensure complete phase separation. The saturated phases were stored at 4 °C in a refrigerator until required.

The shake-flask procedure was conducted in amber 2-mL HPLC vials. A volume of 300 μL of the working solution (2.5 μg mL^{-1}) was combined with 1500 μL of *n*-octanol pre-saturated with PBS. To minimise material loss due to volatilisation, the volume of the two-phase system was adjusted to nearly fill the vials. The *n*-octanol-buffer mixtures were vortexed for 1 minute, followed by shaking for 1 hour at 150 oscillations per minute and 25.0 ± 0.1 °C to achieve equilibrium and phase distribution. Subsequently, the samples were centrifuged in a tabletop centrifuge at 4000×*g* for 30 minutes at 25 °C to ensure the removal of any emulsions.

Sample analysis. – The vials were placed in the autosampler rack maintained at 25 °C, with an injection volume of 10 μL and a needle offset of 0.5 mm. To prevent carryover from the *n*-octanol phase, the syringe exterior was thoroughly washed with methanol after each injection. Chromatographic analysis was performed on a Zorbax SB C18 column (150 mm length, 4.6 mm inner diameter, 5 μm particle size) equipped with a safety guard column (Agilent Technologies). The analysis was conducted in isocratic mode at 25.0 ± 0.1 °C within a 10-min runtime. The mobile phase consisted of a methanol/water mixture (60/40, *V/V*) with 0.1 % formic acid as a modifier. The mobile phase was filtered using a membrane filter (No. 66, diameter 47 mm, pore size 0.45 μm; Supelco, USA) prior to use and delivered at a flow rate of 1.0 mL min^{-1}. Absorbance spectra were recorded in the wavelength range of 200–400 nm during the chromatographic runs, with detection wavelengths set to 295 nm for aloin A and 280 nm for aloe-emodin.

Method validation. – The method was validated for the determination of aloin A and aloe-emodin following the guidelines of the International Council for Harmonization of Technical Requirements for Pharmaceuticals for Human Use (ICH), as outlined in the *Validation of Analytical Procedures ICH Q2(R2)* (19).

Chromatographic methods

Sample preparation. – Stock solutions of the analytes were prepared by dissolving 10 mg of each compound in 10 mL of methanol and stored at 4 °C. Working solutions were freshly prepared daily by diluting the stock solutions to a concentration of 100 μg mL^{-1} using methanol. Before use, all samples were sonicated for 10 minutes at 25 °C in an ultrasonic bath and filtered through 0.2-μm polyethersulfone filters (Obrnuta faza). Amber glass HPLC vials were utilised to protect the analytes from photodegradation.

RP-TLC analysis. – The chromatographic behaviour of aloin A and aloe-emodin was investigated using RP-18 plates (dimensions 10 × 10 cm) with a fluorescent indicator (Merck). Working solutions (100 μg mL^{-1}) were applied to the plates using a 10-μL syringe (Hamilton Company, Switzerland) in 5-mm wide bands, positioned 10 mm from the bottom edge and 15 mm from the sides of the plates. Mobile phases were prepared by mixing

PBS (20 mmol L^{-1}, pH 7.4) with methanol, varying the organic solvent content from 50 to 80 % in 5 % increments. A vertical flat-bottom development chamber (Camag) with a stainless-steel lid was pre-saturated with the mobile phase for 30 minutes. Plates were developed over a distance of 9 cm at room temperature and subsequently air-dried for 5 minutes. Analyte visualisation was conducted under UV light at a wavelength of 254 nm using a UV cabinet.

RP- and IAM-HPLC analysis. – RP C18-HPLC analysis was performed using a Zorbax SB C18 chromatographic column (150 mm length, 4.6 mm inner diameter, 5 μm particle size) with a safety guard column from Agilent Technologies.

IAM-HPLC analysis was conducted using an IAM.PC.DD2 chromatographic column (50 mm length, 3.0 mm inner diameter, 10-μm particle size) with a safety guard column by Regis Technologies (USA).

The injection volume was set to 10 μL, and all of the measurements were performed at 25.0 ± 0.1 °C using an isocratic elution method.

The flow rate was maintained at 1.0 mL min^{-1}. The mobile phases consisted of mixtures of PBS (20 mmol L^{-1}, pH 7.4) and methanol, with the organic solvent content varying from 50 to 80 % in 5 % increments for RP C18-HPLC assay and from 35 to 55 % in 5 % increments for IAM-HPLC assay. The mobile phases were filtered using a membrane filter (No. 66, diameter 47 mm, pore size 0.45 μm; Supelco) prior to use.

The retention time of the unretained solute (t_0) was determined by injecting a sodium nitrate solution (0.1 mg mL^{-1} in the mobile phase). Retention times were recorded at wavelengths of 295 nm for aloin A and 280 nm for aloe-emodin.

HSA- and AGP-HPLC analysis. – The interaction of aloin A and aloe-emodin with plasma proteins was analysed using affinity chromatography with columns provided by Chrom-Tech (France). Two types of immobilised protein columns were employed: human serum albumin (HSA) (Chiralpak-HSA, 50 mm length, 4.6 mm inner diameter, 5-μm particle size) and α1-acid glycoprotein (AGP) (Chiralpak-AGP, 50 mm length, 4.6 mm inner diameter, 5-μm particle size). The injection volume was set to 10 μL.

The mobile phase consisted of 20 mmol L^{-1} potassium phosphate buffer (pH 7.4) as phase A and *i*-propanol as phase B. A linear gradient from 0 to 30 % *i*-propanol was applied from 0 to 6 min, held *i*-propanol at 30 % for 9 minutes, and then returned to pure potassium phosphate solution. The flow rate of the mobile phase was maintained at 1.5 mL min^{-1} throughout the experiment. A five-minute column recalibration was performed between each run. All experiments were conducted at a controlled temperature of 25.0 ± 0.1 °C. Retention times were recorded at wavelengths of 295 nm for aloin A and 280 nm for aloe-emodin.

RESULTS AND DISCUSSION

In silico *prediction of physicochemical properties, ADME and drug-likeness profiles*

The physicochemical and ADME properties of active compounds are critical factors for successful drug development. Computational approaches for their evaluation offer

several advantages over experimental methods, including rapid calculation times, low cost and environmental friendliness. Additionally, computational methods enable the prediction of these properties before synthesis, making them particularly relevant for designing putative drug molecules. Many software tools are available to estimate the physicochemical and ADME properties using various algorithms. However, it is important to note that numerous studies have reported substantial discrepancies between the calculated values and the experimentally determined ones. Estimated values are often inaccurate, and the reliability of calculation methods is particularly low for highly complex compounds. Therefore, various computational approaches, based on different algorithms, were utilised to provide a comprehensive understanding of these properties.

As a starting point for the *in silico* study, we used SwissADME software to assess the oral drug-likeness of aloin A and aloe-emodin according to the rules established by Lipinski, Ghose, Veber, Egan, and Muegge (20, 24). Aloe-emodin complies with Lipinski's rule of five, featuring three hydrogen bond donors (acceptable if less than five), five hydrogen bond acceptors (acceptable if less than ten), molecular mass of 270 Da (acceptable if less than 500 Da), and MLOGP value of 0.1 (acceptable if less than five). In recent studies, researchers have further explored the relationship between physicochemical properties and their impact on drug-likeness, leading to the development of additional criteria that complement Lipinski's rule. These rules include the number of rotatable bonds, as molecular rigidity is closely linked to bioavailability. It has also been proposed that the number of hydrogen bonding groups should be replaced by the TPSA as a descriptor for evaluating the percentage of oral intestinal absorption of a drug, as they are inversely proportional. Consequently, aloe-emodin is expected to exhibit high oral bioavailability with a TPSA below 140 $Å^2$ (calculated values ranged from 76.39 to 113.28 $Å^2$) and one rotatable bond (acceptable if less than 10) (Table I) whereas aloin A failed to comply with Lipinski's rule of five, due to having seven hydrogen bond donors. It also failed to conform to Ghose's rule because of a negative WLOGP value. Additional oral drug-likeness evaluation approaches indicated unacceptable oral bioavailability, attributed to its high TPSA values (calculated to the range from 135.25 to 170.60 $Å^2$) (Table I). A recent study by Bultum and co-workers (18) revealed that 2 or 3 violations of drug-likeness rules are common among oral phytochemicals and their derivatives. Therefore, both aloin A and aloe-emodin demonstrated generally acceptable drug-likeness and physicochemical characteristics.

Lipophilicity, expressed as the logarithm of the partition coefficient between *n*-octanol and the aqueous phase (log *P*), is a key physicochemical property that significantly influences various pharmacokinetic parameters. The calculated log *P* values for aloin A and aloe-emodin are summarised in Table I. Based on theoretical predictions, aloin A is classified as a hydrophilic compound, with an average predicted log *P* value of –0.38 (standard deviation of 0.74). In contrast, aloe-emodin is characterised as a hydrophobic compound, with an average predicted log *P* value of 1.73 (standard deviation of 0.61). Discrepancies in the computed log *P* values are apparent for both molecules, with substantial variations noted in specific cases: aloin A shows a substantial difference of 2.99 between the iLOGP (1.40) and MLOGP (–1.59) descriptors, while aloe-emodin exhibits a disparity of 2.32 between miLogP (2.42) and MLOGP (0.1). It is highly likely that theoretical approaches differentiate the log *P* values of aloin A and aloe-emodin, as the hydrophilic sugar moiety (β-ᴅ-glucopyranosyl unit) attached at the C-10 position is expected to decrease the log *P* value of aloin, the C-glucoside derivative of aloe-emodin (we calculated log *P* value

Table I. Summary of physicochemical properties obtained by theoretical approaches

Software/source	Abbreviation	Aloin A	Aloe-emodin
Lipophilicity[a]			
Swiss ADME	iLOGP	1.40	1.96
Swiss ADME	XLOGP3	−0.12	1.82
Swiss ADME	WLOGP	−1.04	1.21
Swiss ADME	MLOGP	−1.59	0.10
Swiss ADME	SILICOS-IT	0.18	2.42
Pubmed	XLogP3-AA	−0.10	1.80
ALOGPS	ALOGPs	−0.49	2.39
Molinspiration	miLogP	0.18	2.42
Mcule	Mcule log P	−0.89	1.37
OSIRIS Property Explorer	cLogP	−1.03	1.74
MolSoft	MolLogP	0.19	2.14
Preadmet QSARHUB	ALOGP98	−0.45	1.67
pkCSM	pkCSM logP	−0.89	1.37
preADMET	SKlog _P	−0.65	1.89
Solubility[b]			
Swiss ADME	$\log S_{SILICOS-IT}$	−1.79	−3.92
Swiss ADME	$\log S_{ESOL}$	−2.46	−3.04
Swiss ADME	$\log S_{ALI}$	−2.95	−3.43
ALOGPS	$\log S_{ALOGPS}$	−2.20	−2.95
OSIRIS Property Explorer	$\log S_{OSIRIS}$	−2.90	−4.02
MolSoft	$\log S_{MolSoft}$	−1.74	−2.59
Preadmet QSARHUB	$\log S_{q\text{-buffer}}$	−3.57	−4.17
Preadmet QSARHUB	$\log S_{q\text{-water}}$	−2.48	−5.00
pkCSM	$\log S_{pkCSM}$	−2.94	−3.10
preADMET	$\log S_{p\text{-buffer}}$	−3.57	−3.98
preADMET	$\log S_{p\text{-water}}$	−2.67	−5.00
admetSAR	$\log S_{admetSAR}$	−2.13	−2.53
Topological polar surface area (Å^2)[c]			
Swiss ADME	$TPSA_{SwissADME}$	167.91	94.83
Molinspiration	$TPSA_{Molinspiration}$	167.90	94.83
Mcule	$TPSA_{Mcule}$	167.91	94.83
OSIRIS Property Explorer	$TPSA_{OSIRIS}$	167.91	94.83
MolSoft	MolPSA	135.25	76.39
pkCSM	PSA_{pkCSM}	170.60	113.28

[a] Lipophilicity is expressed as the logarithm of the partition coefficient of a compound between *n*-octanol and aqueous phase (log *P*).

[b] Solubility is expressed as the logarithm of the concentration of a compound in mol L^{-1} for a saturated aqueous solution (log *S*).

[c] Topological polar surface area is defined as the sum of the surfaces of polar atoms in a molecule.

of β-ᴅ-glucopyranose and its average log P is –2.16). All theoretical approaches successfully distinguished the log P values of aloin A and aloe-emodin ($1.69 \leq \Delta_{\log P} \leq 2.88$) except iLOGP ($\Delta_{iLOGP} = 0.56$). It is noteworthy that the calculated iLOGP value for aloin A is several times higher than those obtained using other approaches. This result can be attributed to the fact that the iLOGP method is based on calculating solvation-free energy, a relatively new theoretical approach for evaluating lipophilicity. Given its novelty, our findings suggest that the iLOGP method requires further refinement.

The solubility of aloin A and aloe emodin, estimated using 12 theoretical approaches, is summarised in Table I and expressed as the logarithm of molar concentration (log S). Both compounds demonstrated suitable solubility. The log S values for aloin A were from –3.57 (log $S_{q\text{-buffer}}$) to –1.79 (log $S_{SILICOS\text{-}IT}$), while for aloe emodin, the values ranged from –5.00 (log $S_{p\text{-water}}$) to –2.53 (log $S_{admetSAR}$). The discrepancies in the computed log S values were 1.83 and 2.47 for aloin A and aloe-emodin, resp.

Table II. Summary of ADME properties obtained by theoretical approaches

Software/source	Abbreviation	Aloin A	Aloe-emodin
Absorption (%)[a]			
Preadmet QSARHUB	HIA$_{QSARHUB}$	33.64	90.64
pkCSM	HIA$_{pkCMS}$	42.80	74.18
preADMET	HIA$_{preADMET}$	33.64	90.64
Skin permeability[b]			
Swiss ADME	log $K_{pSwissADME}$	–8.94	–6.66
Preadmet QSARHUB	log $K_{pQSARHUB}$	–8.27	–7.97
pkCSM	log K_{ppkCSM}	–2.74	–2.74
preADMET	log $K_{preADMET}$	–8.27	–7.97
Plasma protein binding (%)[c]			
Preadmet QSARHUB	PPB$_{QSARHUB}$	50.09	91.11
preADMET	PPB$_{preADMET}$	50.09	91.11
Blood-brain barrier premeability[d]			
MolSoft	BBB$_{MolSoft}$	1.75	2.93
Preadmet QSARHUB	BBB$_{QSARHUB}$	0.05	0.49
pkCSM	BBB$_{pkCSM}$	0.09	0.19
preADMET	BBB$_{preADMET}$	0.05	0.49
admetSAR	BBB$_{admetSAR}$	0.69	0.74

[a] Human intestinal absorption is expressed as a numerical value that represents the percentage of absorbed drug.

[b] Skin permeability is expressed as the logarithm of the permeability rate at cm s^{-1}.

[c] Plasma protein binding is expressed as 'fraction bound', *i.e.*, the ratio of bound concentration over the total concentration of the drug in the bloodstream.

[d] Blood-brain barrier permeability is expressed as the drug concentration in the brain divided by the concentration in the blood.

Following the evaluation of physicochemical properties, we proceeded with the prediction of ADME properties for aloin A and aloe-emodin using six computational platforms (Table II). The well-established preADMET platform was employed alongside two innovative approaches: pkCSM, which utilises graph-based signatures, and admetSAR, which is based on models trained using advanced machine learning techniques. Additionally, SwissADME was applied to predict skin permeability based on the QSPR model established by Potts and Guy (25), while MolSoft, utilising the internal coordinate mechanics approach, was used for the evaluation of blood-brain barrier permeability. The ADME data obtained from the preADMET QSARHUB platform were identical to those from the preADMET approach, suggesting that both platforms rely on the same theoretical framework.

As mentioned by Sánchez-Machado and co-workers (26), aloe is used as a laxative due to its ability to reduce intestinal absorption of water. Both anthraquinones, aloin A and aloe-emodin, are associated with the purgative action of aloe. Although the mechanisms regulating the balance of these various effects are poorly understood, information on their intestinal absorption can provide insight into the appropriate oral dosage needed to achieve the desired physiological activity *in vivo*. The ADME property HIA describes the process by which orally administered drugs are absorbed from the gastrointestinal system into the bloodstream. Comparable HIA values were obtained using both theoretical approaches (ranging from 33.64 to 42.80 % for aloin and from 74.18 to 90.64 % for aloe-emodin), revealing that the predicted intestinal absorption of aloe-emodin is approximately twofold higher than that of aloin A. Notably, the values obtained were more than six times higher for aloin A and eight times higher for aloe-emodin compared to those reported in the study by Park and co-workers (27).

Aloe is commonly used to treat various skin conditions, such as dry skin and irritant contact dermatitis, as well as to promote the healing of burns. Recent insights into the broad pharmacological properties of aloin and aloe-emodin, including their anticancer, anti-inflammatory, antiviral, and antibacterial activities, have supported the idea of incorporating aloin A and aloe-emodin into functional skincare products. Suitable skin permeability is essential for their effective transdermal delivery. However, data on the ability of anthraquinones to penetrate the skin barrier is lacking, and the safety of topical aloe applications, particularly concerning systemic toxicity, has not been fully evaluated (28). The calculated skin permeability of aloin A and aloe-emodin offers valuable insight into their potential to penetrate the skin (Table II). Regarding the skin permeability data, a discrepancy was observed between the values obtained from various theoretical approaches. Notably, two out of three theoretical approaches predicted log K_p values lower than −8.27 and −6.66 cm s^{-1} for aloin A and aloe-emodin, resp. These log K_p values are lower than those reported for common transdermal drugs (the average SwissADME log K_p value is −4.5 cm s^{-1}), indicating a reduced permeation potential for the investigated phytochemicals. These low log K_p values indicate very low permeability, suggesting that these phytochemicals are unlikely to pass through the skin in sufficient quantities to achieve therapeutic effects without significant enhancement strategies, such as the use of chemical permeation enhancers or microneedles (29).

Two major plasma proteins in humans, HSA and AGP, are primarily responsible for binding endobiotics and xenobiotics. It is widely recognised that acidic compounds exhibit a higher affinity for HSA, whereas AGP predominantly binds to neutral and basic com-

pounds. Bi and co-workers (30) reported that anthraquinones interact with HSA by forming complexes, which supports the data obtained in our *in silico* study. A higher affinity for plasma proteins was proposed for aloe-emodin than for its C-glucoside (Δ_{PPB} = 40 %).

The blood-brain barrier is a selective, multicellular, dynamic, and semipermeable boundary that maintains homeostasis within the central nervous system by protecting it from external compounds. All theoretical approaches, except for MolSoft, estimated BBB values close to zero, with predictions not exceeding 0.74, indicating poor permeability of aloin A and aloe-emodin across the blood-brain barrier. In contrast, MolSoft predicted significantly higher BBB values of 1.75 and 2.93 for aloin A and aloe-emodin, resp. As expected, aloin A exhibited lower BBB values compared to aloe-emodin, likely due to its larger molecular size, lower lipophilicity, and glycosidic structure ($0.05 \le \Delta_{BBB} \le 1.18$).

The *in silico* data obtained for aloin A and aloe-emodin served as the foundation for designing experiments to assess lipophilicity, hydrophobicity, and biomimetic chromatography profiles.

Shake-flask data

Following the in silico study, the next phase of our research focused on experimental techniques for determining the lipophilicity of aloin A and aloe-emodin. The traditional *n*-octanol-determined shake-flask method, a gold standard for log *P* determination, was used to obtain scalable and easily transferable results. In our previous studies, we developed and successfully applied a semi-automated, miniaturised shake-flask methodology combined with rapid chromatographic analysis to investigate the lipophilicity of a wide range of drugs and phytochemicals used in the treatment of inflammatory bowel disease (12, 13, 31). Thus, this advanced methodology was adapted to evaluate the lipophilicity of aloin A and aloe-emodin.

The HPLC technique was first evaluated to confirm its suitability for the intended analytical application and to ensure reproducibility. Standard solutions containing aloin A and aloe-emodin (2.5 µg mL^{-1}) were analysed in six replicates. The results, summarised in Table III, include key parameters such as retention time, peak area, peak purity, retention factor, peak symmetry and theoretical plate count. The observed retention times for aloin A and aloe-emodin were 4.10 and 4.08 min, resp. The total method run time of 5 minutes makes the procedure both time-efficient and cost-effective. Statistical analysis revealed no significant deviations in system suitability data. The relative standard deviation (RSD) values for all evaluated parameters were below 4.4 %, demonstrating that the analytical procedure complies with ICH and USP (United States Pharmacopoeia) standards.

Subsequent investigations focused on validating the analytical procedure for aloin A and aloe-emodin following ICH guidelines (19). The method was validated for various parameters, including linearity, limit of detection (*LOD*), limit of quantitation (*LOQ*), precision, accuracy, and standard solution stability (Table III).

Standard solutions ranging from 0.1 to 5.0 µg mL^{-1} were prepared to construct calibration curves for linearity assessment. The high correlation coefficients (*R* = 0.999 for both aloin A and aloe-emodin) confirm the strong linearity of the method across the specified concentration range (Fig. S1 in the Supplementary material).

Table III. Shake-flask method system suitability and validation data

Parameter	Aloin A	Aloe-emodin	Reference value(s)
System suitability (*n* = 6)[a]			
Retention time (min; RSD, %)	4.10; 0.7	4.08; 0.4	RSD < 2.0
Peak area (mAU s; RSD, %)	153.7; 0.3	79.3; 0.4	RSD < 2.0
Peak purity (value; RSD, %)	999.1; 1.5	999.2; 2.4	> 999.0
Retention factor (value; RSD, %)	2.15; 1.0	2.14; 0.6	2–8
Symmetry (value; RSD, %)	0.92; 4.4	0.98; 2.6	0.8–1.2
Theoretical plate count (value; RSD, %)	42662; 1.8	40687; 1.9	>1500; RSD < 2.0
Linearity (*n = 5*)			
Range (µg mL^{-1})	0.1–5	0.1–5	N/A
Slope	59.51	29.83	N/A
Intercept	−0.206	−0.215	N/A
Standard error of slope	0.104	0.088	N/A
Standard error of the intercept	0.230	0.209	N/A
Correlation coefficient (*R*)	0.999	0.999	>0.990
Regression sum of squares	44,776	11,937	N/A
Residual sum of squares	0.550	0.315	N/A
Total sum of squares	44,777	11,937	N/A
Slope – lower 95 % confidence interval	59.22	29.55	N/A
Slope – higher 95 % confidence interval	59.79	30.11	N/A
Intercept – lower 95 % confidence interval	−0.844	−0.879	N/A
Intercept – higher 95 % confidence interval	0.432	0.449	N/A
Sensitivity[b]			
Limit of detection (µg mL^{-1})	0.05	0.05	N/A
Limit of quantitation (µg mL^{-1})	0.1	0.1	N/A
Precision[c]			
Repeatability (*n* = 6; RSD, %)	0.4	1.0	RSD < 2.0
Intermediate precision (*n* = 18; RSD, %)	0.2	0.8	RSD < 2.0
Accuracy (*n* = 3)[d]			
Low level (mean recovery, %; RSD, %)	99.7; 1.3	104.5; 1.8	95–105; RSD < 2.0
Medium level (mean recovery, %; RSD, %)	100.8; 0.3	99.5; 0.4	95–105; RSD < 2.0
High level (mean recovery, %; RSD, %)	103.8; 0.1	102.0; 1.1	95–105; RSD < 2.0

Stability[e]			
Benchtop stability (recovery, %)	99.5	100.0	95–105
Short-term stability (recovery, %)	100.6	99.1	95–105
Long-term stability (recovery, %)	100.2	97.7	95–105

N/A – not applicable, RSD – relative standard deviation

[a] System suitability data were obtained using standard solutions of aloin A and aloe-emodin (2.5 µg mL^{-1}).

[b] The limits of detection (*LOD*) and quantitation (*LOQ*) were determined by diluting the standard solutions of aloin A and aloe-emodin, based on signal-to-noise ratio of 3:1 and 10:1, resp.

[c] Repeatability was assessed by analysing the standard solutions of aloin A and aloe-emodin (2.5 µg mL^{-1}) within the same day in six replicates, while the intermediate precision was evaluated by analysing the standard solutions on three consecutive days, also in six replicates.

[d] Accuracy was evaluated by analysing standard solutions (0.5, 2.5, and 5 µg mL^{-1}) in triplicate.

[e] The stability of the standard solutions of aloin A and aloe-emodin (2.5 µg mL^{-1}) was assessed under different conditions: at room temperature for 8 hours (benchtop stability), at 4 °C for 3 days (short-term stability), and at –20 °C for 7 days (long-term stability).

The *LOD* and *LOQ* values, representing analyte concentrations corresponding to signal-to-noise ratios of 3 and 10, resp., were determined to be 0.05 µg mL^{-1} and 0.1 µg mL^{-1}.

Method precision was evaluated for repeatability (intra-day precision) by analysing six replicates of 2.5 µg mL^{-1} standard solutions within the same day and for intermediate precision (inter-day precision) by comparing results obtained on three consecutive days (Fig. S2 in the Supplementary materials). All RSD values were below 1.0 %, demonstrating excellent precision, as shown in Table III.

Accuracy was assessed using percentage recoveries at three concentration levels (0.5, 2.5, and 5.0 µg mL^{-1}) along the linearity range, calculated using the regression equation. The recoveries ranged from 99.7 to 103.8 % (RSD ≤ 1.3 %) for aloin A and from 99.5 to 104.5 % (RSD ≤ 1.8 %) for aloe-emodin, indicating the method's acceptable accuracy (Table III).

Stability experiments were conducted using standard solutions of aloin A and aloe-emodin (2.5 µg mL^{-1}) under different conditions, including benchtop, autosampler, and long-term stability tests. Recoveries ranged between 97.7 and 100.6 %, confirming the sufficient stability of the solutions under all tested conditions.

The optimised shake-flask method was successfully employed to determine the log *P* values of aloin A and aloe-emodin (Table IV). As anticipated, the log *P* values were closely

Table IV. Shake-flask data

Compound	log *P*	RSD (%)[a]
Aloin A	0.07	4.8
Aloe-emodin	1.31	4.6

RSD – relative standard deviation

[a] *n* = 3

associated with the chemical structure of these phytochemicals. Aloin A was found to be more hydrophilic than aloe-emodin, likely due to the presence of an attached β-ᴅ-gluco-pyranosyl unit ($\Delta_{\log P}$ = 1.24). The experimentally obtained data were compared with those predicted by various theoretical approaches. Analysis revealed minimal differences between the experimental values and the average calculated values for both compounds, with discrepancies of less than 0.45.

Reversed-phase thin-layer chromatographic data

Parallel to the traditional shake-flask method, thin-layer chromatography (TLC) was utilised to determine the lipophilicity of aloin A and aloe-emodin (Table V). After developing chromatographic plates with mobile phases consisting of methanol and PBS, spot positions were recorded, and retention factors (R_F) were calculated. The R_F values ranged from 0.24 to 0.68 for aloin A and from 0.10 to 0.34 for aloe-emodin (Fig. S3 in the Supplementary material). The narrower range observed for aloe-emodin can be attributed to its higher affinity for the stationary phase. Afterwards, the R_M values were calculated using the equation: $R_M = \log[(1/R_F) - 1]$. It was observed that the R_M values decreased with an increasing concentration of organic modifier in the mobile phase, ranging from 0.51 to −0.32 for aloin A and from 1.13 to 0.29 for aloe-emodin. Based on the linear relationship between R_M and the concentration of the organic modifier, the R_{M0} values were deter-

Table V. RP-TLC data

Parameter	Aloin A	Aloe-emodin
Range of organic solvent content (%)	50–80	55–80
R_F	0.24–0.68	0.10–0.34
R_{Mw}	1.85	3.06
Linearity[a]		
Slope	−0.027	−0.035
Intercept	1.853	3.058
Slope – lower 95 % confidence interval	−0.029	−0.038
Slope – higher 95 % confidence interval	−0.025	−0.032
Intercept – lower 95 % confidence interval	1.70	2.89
Intercept – higher 95 % confidence interval	2.00	3.23
Standard error of slope	0.001	0.001
Standard error of the intercept	0.059	0.068
Correlation coefficient (R)	0.995	0.996
Regression sum of squares	0.517	0.852
Residual sum of squares	0.003	0.004
Total sum of squares	0.520	0.856

[a] Number of calibration points: 7 (aloin A) and 6 (aloe-emodin).

mined by extrapolating the organic modifier concentration to zero. The high correlation coefficients between R_M and concentration of methanol in the mobile phase (φ) (0.995 for aloin A and 0.996 for aloe-emodin) confirm the linearity of the method, allowing for accurate determination of R_{M0} values by *y*-axis extrapolation. The RP-TLC lipophilicity index, R_{M0}, was higher for aloe-emodin compared to aloin A, which is consistent with their log *P* shake-flask values ($\Delta_{R_{M0}}$ = 1.21).

Reversed-phase high-performance liquid chromatographic data

To further evaluate the lipophilicity of aloin A and aloe-emodin, an HPLC method using an octadecyl silyl silica gel stationary phase was employed, which is recognised as a mainstream experimental method for lipophilicity determination (Table VI). Lipophilicity determination by RP-HPLC is based on the logarithm of the retention factor (log *k*), calculated using the formula log k = log$(t_R - t_0)/t_0$, where t_R is the analyte retention time and t_0 corresponds to the dead time. Direct measurement of log *k* in PBS for both phytochemicals, aloin A and aloe-emodin, was not feasible due to their high affinity for the stationary phase, resulting in rather long retention times and extensive peak broadening. To address this issue, the percentage of organic modifier in the mobile phase was optimised to ensure retention times within 15 minutes while maintaining acceptable peak shapes (Fig. S4 and

Table VI. RP-HPLC data

Parameter	Aloin A	Aloe-emodin
Range of organic solvent content (%)	50–80	50–80
Retention time, t_R (min)	2.92–6.02	3.89–14.22
log k_w^{C18}	1.37	3.02
φ_0^{C18}	68.50	81.62
Linearity[a]		
Slope	−0.020	−0.037
Intercept	1.373	3.015
Slope – lower 95 % confidence interval	−0.023	−0.045
Slope – higher 95 % confidence interval	−0.017	−0.030
Intercept – lower 95 % confidence interval	1.16	2.52
Intercept – higher 95 % confidence interval	1.59	3.50
Standard error of slope	0.001	0.002
Standard error of the intercept	0.078	0.154
Correlation coefficient (*R*)	0.993	0.995
Regression sum of squares	0.230	0.742
Residual sum of squares	0.003	0.008
Total sum of squares	0.233	0.750

[a] Number of calibration points: 7 (aloin A and aloe-emodin).

Fig. S5 in the Supplementary material). Under suitable isocratic chromatographic conditions, the retention times of aloin A and aloe-emodin ranged from 2.92 to 14.22 minutes, with peak asymmetry factors between 0.8 and 1.2. Based on the linear relationship between log k values and the concentration of organic modifier in the mobile phase, the RP-HPLC lipophilicity index, log k_w^{C18}, was determined by extrapolating the organic modifier concentration to zero. High correlation coefficients (R values were 0.993 and 0.995 for aloin A and aloe-emodin, resp.) confirmed a good correlation between organic modifier concentration and log k values. Additionally, another RP-HPLC lipophilicity index, φ_0^{C18}, introduced by Valkó and Slégel (32), was implemented in this study. This index represents the volume fraction of the organic modifier in the mobile phase at which equal partitioning of the solute between the mobile and stationary phases occurs. Both RP-HPLC indices, lipophilicity index (log k_w^{C18}) and hydrophobicity index φ_0^{C18}, were higher for aloe-emodin compared to aloin A, aligning with their log P (obtained through *in silico* and shake-flask methods) and R_{M0} values ($\Delta_{\log k_w C18}$ = 1.65 and $\Delta_{\varphi_0 C18}$ = 13.12).

Immobilised artificial membrane chromatographic data

Biomimetic chromatographic techniques provide a valuable alternative for assessing ADME properties of various drugs and biologically active compounds. IAM stationary phases, based on monolayers of phospholipids covalently bound to a propylamine-silica core, are employed in reversed-phase HPLC. These stationary phases offer a simplified model of complex lipoidal biological bilayers, with two primary limitations: the monolayered nature of the membrane and the use of only a single phospholipid type in stationary phase preparation. The analytical procedure used to determine the lipophilicity index, log k_0^{IAM}, follows the principles for C18-HPLC assay (Table VII). As in the C18-HPLC assay, the percentage of organic modifier in the mobile phase was optimised to ensure retention times within 15 minutes while maintaining acceptable peak shapes. However, compared to the C18-HPLC assay, a lower concentration of organic modifier in the mobile phase was required to achieve suitable retention times for the investigated phytochemicals, reflecting differences in interaction with the IAM stationary phase. Under isocratic chromatographic conditions outlined in Table VII the retention times of aloin A and aloe-emodin ranged from 0.89 to 10.30 min with peak asymmetry factors between 0.8 and 1.2. The IAM-HPLC lipophilicity index, log k_w^{IAM}, was determined by extrapolating the organic modifier concentration in the mobile phase to zero, based on the linear relationship between log k values and the organic modifier concentration. The high correlation coefficients (R = 0.999 for aloin A and R = 0.993 for aloe-emodin) indicate suitable linearity between the log k values and the organic modifier concentration. Both aloin A and aloe-emodin demonstrated lower retention on the IAM column compared to the C18 column; however, the calculated log k_w^{IAM} values were higher than the log k_w^{C18} values, with differences of up to 1.5 units. A similar trend was observed in our previous studies of various phytochemicals, including boswellic acids, curcumins, and andrographolides (12). Furthermore, unlike aloe-emodin, the presence of a sugar moiety (β-ᴅ-glucopyranosyl unit) at the C-10 position of aloin A considerably enhanced its affinity to phospholipids ($\Delta_{\log k_w IAM}$ = 0.37) compared to its affinity to alkyl chains ($\Delta_{\log k_w C18}$ = 1.65 and $\Delta_{R_{M0}}$ = 1.21). Additionally, the volumes of organic modifier in the mobile phase required for equal partitioning of aloin A and aloe-emodin between the mobile phase and the IAM stationary phase were lower than those obtained using the C18-HPLC assay (up to 20.6 %) and exhibited slightly higher

differences ($\Delta_{\varphi_0 IAM}$ = 18.17). These findings suggest that unlikely partitioning in *n*-octanol/water system or C18 chains, partition into phospholipids involved not only hydrophobic intermolecular recognition forces but also electrostatic interactions.

Table VII. IAM-HPLC data

Parameter	Aloin A	Aloe-emodin
Range of organic solvent content (%)	35–50	35–65
Retention time, t_R (min)	0.89–6.42	1.94–10.30
log k_w^{IAM}	2.87	3.24
φ_0^{IAM}	47.93	66.10
Linearity[a]		
Slope	−0.060	−0.049
Intercept	2.873	3.239
Slope – lower 95 % confidence interval	−0.067	−0.060
Slope – higher 95 % confidence interval	−0.058	−0.038
Intercept – lower 95 % confidence interval	2.82	2.77
Intercept – higher 95 % confidence interval	3.18	3.71
Standard error of slope	0.001	0.003
Standard error of the intercept	0.042	0.148
Correlation coefficient (*R*)	0.999	0.993
Regression sum of squares	0.855	1.039
Residual sum of squares	0.001	0.015
Total sum of squares	0.855	1.054

[a] Number of calibration points: 7 (aloin A) and 6 (aloe-emodin).

Plasma protein binding data

The biomimetic stationary phases with immobilised proteins HSA and AGP were used to estimate the affinity of aloin A and aloe-emodin to plasma proteins. The standardisation and verification of HSA and AGP assays, using a calibration set of compounds, are detailed in our previously published study (10). These assays were successfully applied for the PPB evaluation of various drugs and phytochemicals (10, 12). For both aloin A and aloe-emodin, higher affinity was observed for HSA than for AGP, with differences in binding proportions of 18.6 % and 13.3 % resp. (Table VIII). Furthermore, glycosylation of dihydroxyanthraquinone at the C-10 position was found to decrease the affinity for both plasma proteins. Specifically, the difference in binding proportions between aloe-emodin and aloin A was 34.8 % for HSA and 40.1 % for AGP. These findings are consistent with our previous research on phytochemicals (curcuminoids, boswellic acids, and andrograph-

pholides used to alleviate inflammatory bowel disease symptoms and phytoestrogens for mitigating menopausal symptoms), which demonstrated a lower affinity for AGP compared to HSA. Additionally, glycosylation of phytoestrogens was shown to reduce their binding affinity for both HSA and AGP (14). The PPB theoretical approach does not differentiate binding for specific proteins; however, the obtained theoretical data were lower than experimentally determined HSA binding values. In contrast, the program overestimated the binding degree for AGP for aloin A and aloe-emodin (see Table II).

Table VIII. HSA- and AGP-HPLC data

Compound	HSA				AGP			
	Retention time (min)	RSD (%)	Binding (%)	RSD (%)[a]	Retention time (min)	RSD (%)	Binding (%)	RSD (%)[a]
Aloin A	1.72	0.1	62.7	0.2	2.20	0.8	44.1	0.7
Aloe-emodin	7.02	0.1	97.5	1.4	5.00	0.2	84.2	0.1

RSD – relative standard deviation

[a] $n = 3$

CONCLUSIONS

This study highlights the distinct pharmacokinetic (absorption and distribution) and physicochemical (solubility and lipophilicity) profiles of aloin A and aloe-emodin, two anthraquinones derived from *Aloe vera*. Aloe-emodin demonstrated superior drug-likeness characteristics, complying with Lipinski's rule of five and exhibiting higher oral bioavailability and intestinal absorption compared to aloin A, which failed to meet certain drug-likeness criteria due to its hydrophilic glycosylated structure. Experimental approaches revealed aloe-emodin as more lipophilic than aloin A, consistent with their molecular structures.

Experimental results confirmed that aloe-emodin has a stronger affinity for plasma proteins compared to aloin A.

The integration of computational and experimental approaches provided a detailed understanding of aloin A and aloe-emodin physicochemical and ADME properties.

Abbreviations, acronyms, symbols. – ADME – absorption, distribution, metabolism, and excretion; AGP – α1-acid glycoprotein; BBB – blood-brain barrier permeability; DMSO – dimethyl sulfoxide; HIA – human intestinal absorption; IAM – immobilized artificial membrane; ICH – International Council for Harmonization of Technical Requirements for Pharmaceuticals for Human Use; *LOD* – limit of detection; log k – logarithm of the retention factor; log k_w^{C18} – RP-HPLC lipophilicity index; log k_w^{IAM} – IAM-HPLC lipophilicity index; log S – the logarithm of molar concentration; log P – logarithm of the partition coefficient; *LOQ* – limit of quantitation; PBS – phosphate buffer saline; PPB – plasma protein binding; R – correlation coefficient; R_F, TLC – retention factor; R_{M0} –TLC lipophilicity index; TPSA – topological polar surface area; φ_0^{C18} – the volume fraction of the organic modifier in the mobile phase at which equal partitioning of the solute between the mobile and stationary phases occurs using RP-HPLC method; φ_0^{IAM} – the volume fraction of the organic modifier in the mobile

phase at which equal partitioning of the solute between the mobile and stationary phases occurs using IAM-HPLC method.

REFERENCES

1. A. Catalano, J. Ceramella, D. Iacopetta, M. Marra, F. Conforti, F. R. Lupi, D. Gabriele, F. Borges and M. S. Sinicropi, *Aloe vera* – An extensive review focused on recent studies, Foods **13** (2024) Article ID 2155 (55 pages); https://doi.org/10.3390/foods13132155

2. S. Kumar, S. Kalita, I. B. Basumatary, S. Kumar, S. Ray and A. Mukherjee, Recent advances in therapeutic and biological activities of *Aloe vera*, *Biocatal. Agric. Biotechnol.* **57** (2024) Article ID 103084 (10 pages); https://doi.org/10.1016/j.bcab.2024.103084

3. K. Khaldoune, N. Fdil and M. Ait Ali, Exploring *Aloe vera*: A comprehensive review on extraction, chemical composition, biological effects, and its utilization in the synthesis of metallic nanoparticles, *Biocatal. Agric. Biotechnol.* **57** (2024) Article ID 103052 (15 pages); https://doi.org/10.1016/j.bcab.2024.103052

4. L. Maduna and A. Patnaik, A review of wound dressings treated with *Aloe vera* and its application on natural fabrics, *J. Nat. Fibers* **20**(1) (2023) Article ID 2190190 (16 pages); https://doi.org/10.1080/15440478.2023.2190190

5. S. Zimbone, V. Romanucci, A. Zarrelli, M. L. Giuffrida, M. F. M. Sciacca, V. Lanza, T. Campagna, L. Maugeri, S. Petralia, G. M. L. Consoli, G. Di Fabio and D. Milardi, Exploring the therapeutic potential of aloin: Unraveling neuroprotective and anticancer mechanisms, and strategies for enhanced stability and delivery, *Sci. Rep.* **14** (2024) Article ID 16731 (12 pages); https://doi.org/10.1038/s41598-024-67397-9

6. N. G. Yoruk and Ö. Istanbullu Paksoy, GC/MS evaluation of the composition of the *Aloe vera* gel and extract, *Food Chemistry: X* **23** (2024) Article ID 101536 (9 pages); https://doi.org/10.1016/j.fochx.2024.101536

7. P. Wang, J. Wei, X. Hua, G. Dong, K. Dziedzic, A. T. Wahab, T. Efferth, W. Sun and P. Ma, Plant anthraquinones: Classification, distribution, biosynthesis, and regulation, *J. Cell. Physiol.* **239**(10) (2024) e31063 (11 pages); https://doi.org/10.1002/jcp.31063

8. K. L. Valko, Biomimetic chromatography – A novel application of the chromatographic principles, *Anal. Sci. Adv.* **3**(3–4) (2022) 146–153; https://doi.org/10.1002/ansa.202200004

9. J. X. Soares, Á. Santos, C. Fernandes and M. M. M. Pinto, Liquid chromatography on the different methods for the determination of lipophilicity: An essential analytical tool in medicinal chemistry, *Chemosensors* **10**(340) (2022) Article ID 340 (41 pages); https://doi.org/10.3390/chemosensors10080340

10. E. Brusač, M.-L. Jeličić, D. Amidžić Klarić, B. Nigović, N. Turk, I. Klarić and A. Mornar, Pharmacokinetic profiling and simultaneous determination of thiopurine immunosuppressants and folic acid by chromatographic methods, *Molecules* **24** (2019) Article ID 3469 (18 pages); https://doi.org/10.3390/molecules24193469

11. M.-L. Jeličić, E. Brusač, D. Amidžić Klarić, B. Nigović, N. Turk and A. Mornar, A chromatographic approach to development of 5-aminosalicylate/folic acid fixed-dose combinations for treatment of Crohn's disease and ulcerative colitis, *Sci. Rep.* **10**(1) (2020) Article ID 20838 (10 pages); https://doi.org/10.1038/s41598-020-77654-2

12. M.-L. Jeličić, D. Amidžić Klarić, J. Kovačić, D. Verbanac and A. Mornar, Accessing lipophilicity and biomimetic chromatography profile of biologically active ingredients of botanicals used in the treatment of inflammatory bowel disease, *Pharmaceuticals* **15**(8) (2022) Article ID 965 (17 pages); https://doi.org/10.3390/ph15080965

13. E. Brusač, M.-L. Jeličić, D. Amidžić Klarić and A. Mornar, Miniaturized shake-flask HPLC method for determination of distribution coefficient of drugs used in inflammatory bowel diseases, *Acta Pharm.* **69**(4) (2019) 649–660; https://doi.org/10.2478/acph-2019-0046

14. K. Lasić, A. Bokulić, A. Milić, B. Nigović and A. Mornar, Lipophilicity and bio-mimetic properties determination of phytoestrogens using ultra-high-performance liquid chromatography, *Biomed. Chromatogr.* **33**(8) (2019) e4551 (13 pages); https://doi.org/10.1002/bmc.4551

15. S. Chatterjee, A. L. Narasimhaiah, S. Kundu and S. Anand, Anti hyperglycaemic study of natural inhibitors for insulin receptor, *Bioinformation* **8**(24) (2012) 1195–1201; https://doi.org/10.6026/97320630081195

16. X. Disalva, M. Sharanya and R. Mahendran, *Aloe vera*: An assured weight loss diet – an approach toward improving the juice palatability and *in silico* analysis, *Asian J. Pharm. Clin. Res.* **12**(6) (2019) 331–336; https://doi.org/10.22159/ajpcr.2019.v12i6.32380

17. S. Das, A. Singh, S. K. Samanta and A. Singha Roy, Naturally occurring anthraquinones as potential inhibitors of SARS-CoV-2 main protease: an integrated computational study, *Biologia* **77** (2022) 1121–1134; https://doi.org/10.1007/s11756-021-01004-4

18. L. E. Bultum, G. B. Tolossa, G. Kim, O. Kwon and D. Lee, *In silico* activity and ADMET profiling of phytochemicals from Ethiopian indigenous aloes using pharmacophore models, *Sci. Rep.* **12** (2022) Article ID 22221 (19 pages); https://doi.org/10.1038/s41598-022-26446-x

19. International Council for Harmonisation of Technical Requirements for Pharmaceuticals for Human Use (ICH), *ICH Q2(R2) Guideline on Validation of Analytical Procedures*, Current Step 5 version, June 2024; https://www.ema.europa.eu/en/documents/scientific-guideline/ich-q2r2-guideline-validation-analytical-procedures-step-5-revision-1_en.pdf; last access date November 14, 2024

20. C. A. Lipinski, F. Lombardo, B. W. Dominy and P. J. Feeney, Experimental and computational approaches to estimate solubility and permeability in drug discovery and development settings, *Adv. Drug Deliv. Rev.* **46**(1–3) (2001) 3–26; https://doi.org/10.1016/s0169-409x(00)00129-0

21. A. K. Ghose, V. N. Viswanadhan and J. J. Wendoloski, A knowledge-based approach in designing combinatorial or medicinal chemistry libraries for drug discovery. 1. A qualitative and quantitative characterization of known drug databases, *J. Comb. Chem.* **1**(1) (1999) 55–68; https://doi.org/10.1021/cc9800071

22. D. F. Veber, S. R. Johnson, H. Y. Cheng, B. R. Smith, K. W. Ward and K. D. Kopple, Molecular properties that influence the oral bioavailability of drug candidates, *J. Med. Chem.* **45**(12) (2002) 2615–2623; https://doi.org/10.1021/jm020017n

23. W. J. Egan, K. M. Merz and J. J. Baldwin, Prediction of drug absorption using multivariate statistics, *J. Med. Chem.* **43**(21) (2000) 3867–3877; https://doi.org/10.1021/jm000292e

24. I. Muegge, S. L. Heald and D. Brittelli, Simple selection criteria for drug-like chemical matter, *J. Med. Chem.* **44**(12) (2001) 1841–1846; https://doi.org/10.1021/jm015507e

25. R. O. Potts and R. H. Guy, Predicting skin permeability, *Pharm. Res.* **9**(5) (1992) 663–669; https://doi.org/10.1023/a:1015810312465

26. D. I. Sánchez-Machado, J. López-Cervantes, R. Sendón and A. Sanches-Silva, *Aloe vera*: Ancient knowledge with new frontiers, *Trends Food Sci. Technol.* **61** (2017) 94–102; https://doi.org/10.1016/j.tifs.2016.12.005

27. M. Y. Park, H. J. Kwon and M. K. Sung, Intestinal absorption of aloin, aloe-emodin, and aloesin; A comparative study using two in vitro absorption models, *Nutr. Res. Pract.* **3**(1) (2009) 9–14; https://doi.org/10.4162/nrp.2009.3.1.9

28. Y. Yang, J.-J. Wu, J. Xia, Y. Wan, J.-F. Xu, L. Zhang, D. Liu, L. Chen, F. Tang, H. Ao and C. Peng, Can aloin develop to medicines or healthcare products? *Biomed. Pharmacother.* **153** (2022) Article ID 113421 (13 pages); https://doi.org/10.1016/j.biopha.2022.113421

29. R. M. Abdallah, H. E. Hasan and A. Hammad, Predictive modeling of skin permeability for molecules: Investigating FDA-approved drug permeability with various AI algorithms, *PLoS Digit. Health* **3**(4) (2024) e0000483 (20 pages); https://doi.org/10.1371/journal.pdig.0000483

30. S. Bi, D. Song, Y. Kan, D. Xu, Y. Tian, X. Zhou and H. Zhang, Spectroscopic characterization of effective components anthraquinones in Chinese medicinal herbs binding with serum albumins, *Spectrochim. Acta A* **62**(1–3) (2005) 203–212; https://doi.org/10.1016/j.saa.2004.12.049

31. M. Medić-Šarić, A. Mornar and I. Jasprica, Lipophilicity study of salicylamide, *Acta Pharm.* **54**(2) (2004) 91–101.

32. K. Valkó and P. Slégel, New chromatographic hydrophobicity index (φ_0) based on the slope and the intercept of the log k' versus organic phase concentration plot, *J. Chromatogr. A* **631**(1–2) (1993) 49–61; https://doi.org/10.1016/0021-9673(93)80506-4

Combined shake-flask, chromatographic, and *in silico* approaches for evaluating the physicochemical and ADME properties of aloin A and aloe-emodin

DANIELA AMIDŽIĆ KLARIĆ, JELENA KOVAČIĆ, PETRA BAJT, NIKŠA TURK, ŽELJKO KRZNARIĆ, EMMA RIORDAN and ANA MORNAR*
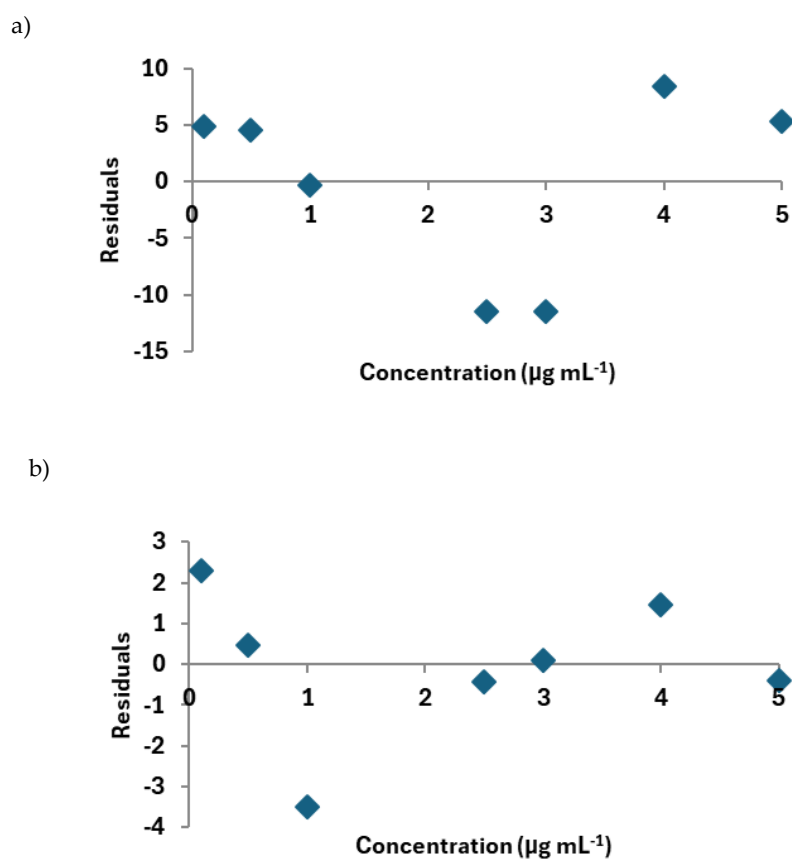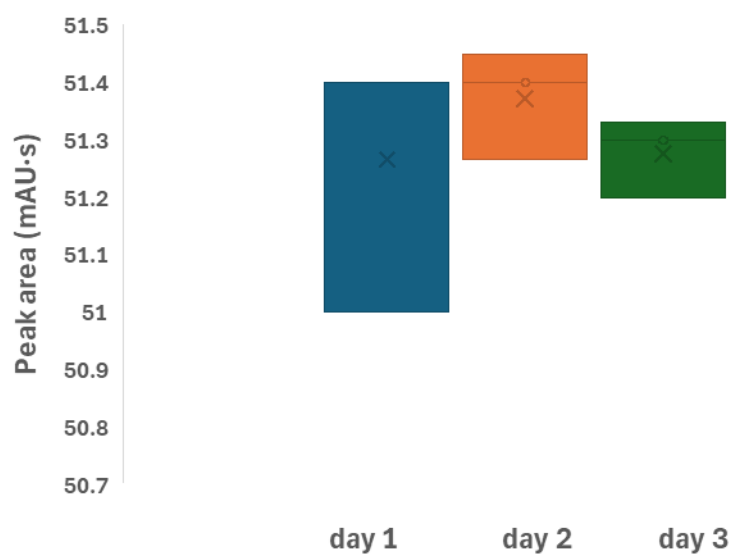
a)

b)

Fig. S1. Residual plots of calibration curves for aloin A (a) and aloe-emodin (b).
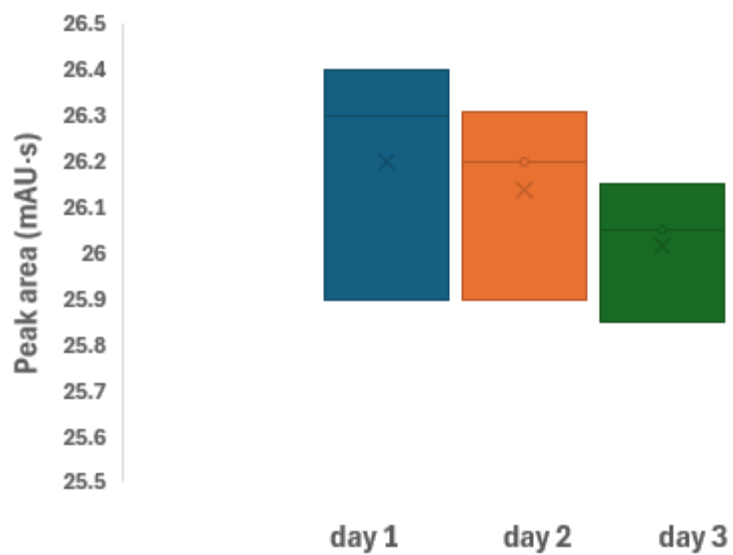
a)

b)

Fig. S2. The box-and-whisker plot of intermediate precision data. The average value is indicated as the cross, the centar line represents the median value, and the large box corresponds to the highest and lowest values, respectively.

Fig. S3. RP-TLC chromatogram (mobile phase was prepared by mixing phosphate buffer saline (20 mM, pH 7.4) with methanol (30:70, V/V); detection – 254 nm; standard solutions – 100 μg mL^{-1}; volume applied – 10 μL). Legend: 1 – aloe-emodin, 2 – aloin A.
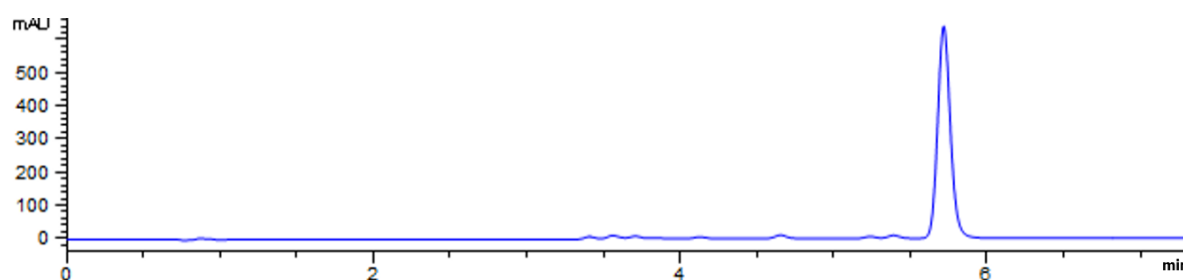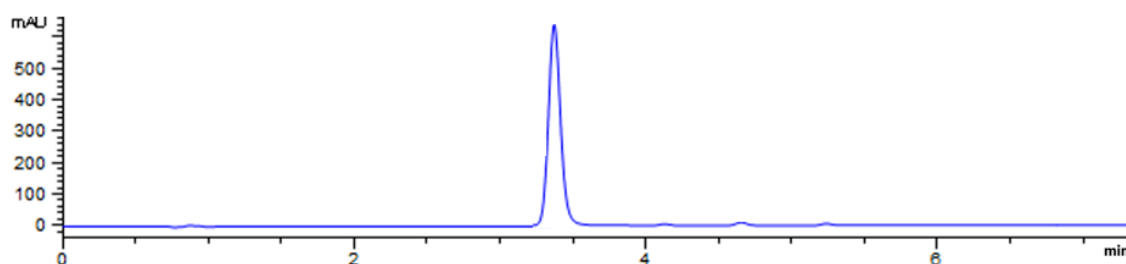

Fig. S4. RP-HPLC chromatogram of aloe-emodin (mobile phases were prepared by mixing phosphate buffer saline (20 mmol L^{-1}, pH 7.4) with methanol (30:70, V/V); detection – 280 nm; standard solutions – 100 μg mL^{-1}; volume of injection – 10 μL; flow – 1 mL min^{-1}).

Fig. S5. RP-HPLC chromatogram of aloin A (mobile phases were prepared by mixing phosphate buffer saline (20 mmol L^{-1}, pH 7.4) with methanol (30:70, V/V); detection – 295 nm; standard solutions – 100 μg mL^{-1}; volume of injection – 10 μL; flow – 1 mL min^{-1}).